# Engineering the Solid State with 2-Benzimidazolones

**ARTICLE** *in* JOURNAL OF THE AMERICAN CHEMICAL SOCIETY · APRIL 1996

Impact Factor: 12.11 · DOI: 10.1021/ja952836l



**4 AUTHORS**, INCLUDING:

John C Macdonald
Worcester Polytechnic Institute
**46** PUBLICATIONS **3,746** CITATIONS

SEE PROFILE

# Engineering the Solid State with 2-Benzimidazolones

**Kathryn E. Schwiebert, Donovan N. Chin, John C. MacDonald, and George M. Whitesides***

*Contribution from the Department of Chemistry, Harvard University, Cambridge, Massachusetts 02138*

*Received August 17, 1995. Revised Manuscript Received February 6, 1996*[⊗]

**Abstract:** Six derivatives of 2-benzimidazolone, disubstituted in the 4 and 5 positions, have been synthesized, and their structures have been determined in the solid state. Four of these compounds crystallize as molecular tapes. Compounds **1-(CH$_3$)$_2$**, **1-Cl$_2$**, and **1-Br$_2$** form tapes that pack with their long axes parallel; compounds **1-H$_2$** and **2-H$_2$** form tapes that pack with their long axes at an angle to one another. Compounds **1-F$_2$** and **1-I$_2$** crystallize with a three-dimensional network of hydrogen bonds. The packing arrangement of molecular tapes is rationalized on the basis of closest packing and electrostatic interactions between aromatic rings. The occurrence of the network motif rather than the tape motif for **1-F$_2$** and **1-I$_2$** is rationalized on the basis of secondary interactions involving the halogen atoms.

## Introduction

This work continues our exploration of the hydrogen-bonded molecular tape as a motif in designing the structures of organic crystals.[1−5] Our objective in this work is to rationalize and predict the structure of molecular crystals from the structures of their constituent molecules. To achieve this goal, we must simplify the structure of organic molecular solids sufficiently that we can understand and control them. Our strategy is to limit the possible orientations of molecules with respect to one another by designing non-covalent interactions into the molecules. We have used molecular tapes—structures in which non-covalent interactions hold molecules in a linear array that is infinite in one dimension—as the central motif in our studies. By constraining molecular aggregates to be tapes, the problem of predicting the packing of molecules simplifies to the problem of predicting the packing of tapes.

Hydrogen-bonding,[6,7] charge-transfer,[8,9] and weak dipole−dipole interactions[10] are non-covalent intermolecular interactions that have been used in efforts to assemble tapes and other structures in the solid state. Hydrogen bonds, in particular, are well suited for building molecular aggregates with specific shapes and sizes because their energies are roughly comparable to thermal energies ($k_bT \approx 0.6$ kcal/mol at 300 K; hydrogen bond energies $\approx 1-5$ kcal/mol) and fairly directional.[6,7,11,12] The design of molecular aggregates using hydrogen bonds to control structure in the solid state has yielded a number of potentially useful structural motifs, including three-dimensional diamondoid networks,[13−15] two-dimensional layers,[16−19] and one-dimensional molecular tapes or rods.[1−5,20−22]

In previous work, we determined the structures of cocrystals of a series of *para*- and *meta*-substituted diphenylmelamines with diethylbarbital (Bar·Mel(PhX)$_2$).[1−3] The strategy in this work was to make a controlled set of modifications of molecular structure and to try to rationalize the differences in the resulting crystalline structures. These molecules cocrystallized in a 1:1 ratio and formed three hydrogen-bonded motifs: "linear" tapes, "crinkled" tapes, and "rosettes" (Figure 1). In this system, we established a correlation between steric interactions between the substituents in the *para* positions and the crystalline motif: as the size of the substituents increased, there was a change from linear to crinkled to rosette motifs. It was difficult to study the effect of the substituents on the *packing* of tapes, however, because substitution could induce a switch from one tape motif to another, rather than simply inducing a change in the packing of the tapes. Polymorphism (the existence of more than one

[⊗] Abstract published in *Advance ACS Abstracts,* March 15, 1996.

(1) Zerkowski, J. A.; Mathias, J. P.; Whitesides, G. M. *J. Am. Chem. Soc.* **1994**, *116*, 4305.
(2) Zerkowski, J. A.; MacDonald, J. C.; Seto, C. T.; Wierda, D. A.; Whitesides, G. M. *J. Am. Chem. Soc.* **1994**, *116*, 2382.
(3) Zerkowski, J. A.; Whitesides, G. M. *J. Am. Chem. Soc.* **1994**, *116*, 4298.
(4) Zerkowski, J. A.; Seto, C. T.; Whitesides, G. M. *J. Am. Chem. Soc.* **1992**, *114*, 5473.
(5) Zerkowski, J. A.; Seto, C. T.; Wierda, D. A.; Whitesides, G. M. *J. Am. Chem. Soc.* **1990**, *112*, 9025.
(6) (a) Chin, D. N.; Zerkowski, J. A.; MacDonald, J. C.; Whitesides, G. M. In *Organised Molecular Assemblies in the Molecular Soid State*; Whitesell, J. T., Ed.; John Wiley & Sons: London, 1995, in press. (b) Desiraju, G. R. *Crystal Engineering: The Design of Organic Solids*; Elsevier: New York, 1989.
(7) Etter, M. C. *J. Phys. Chem.* **1991**, *95*, 4601.
(8) Fagan, P. J.; Ward, M. O.; Calabrese, J. C. *J. Am. Chem. Soc.* **1989**, *111*, 1698.
(9) Ward, M. D.; Fagan, P. J.; Calabrese, J. C.; Johnson, D. C. *J. Am. Chem. Soc.* **1989**, *111*, 1719.
(10) Reddy, D. S.; Panneerselvan, K.; Pilati, T.; Desiraju, G. R. *J. Chem. Soc., Chem. Commun.* **1993**, 661.
(11) Aakeroy, C. B.; Seddon, K. R. *Chem. Soc. Rev.* **1993**, *22*, 397.
(12) Jeffrey, G. A.; Saenger, W. *Hydrogen Bonding in Biological Structures*; Springer-Verlag: Berlin, 1991.
(13) Ermer, O.; Eling, A. *J. Chem. Soc., Perkin Trans. 2* **1994**, 925.
(14) Wang, X.; Simard, M.; Wuest, J. D. *J. Am. Chem. Soc.* **1994**, *116*, 12119.
(15) Zaworotko, M. J. *Chem. Soc. Rev.* **1994**, *23*, 283.
(16) Zhao, X.; Chang, Y.-L.; Fowler, F. W.; Laugher, J. W. *J. Am. Chem. Soc.* **1990**, *112*, 6627.
(17) Chang, Y.-L.; West, M.-A.; Fowler, F. W.; Laugher, J. W. *J. Am. Chem. Soc.* **1993**, *115*, 5991.
(18) Hollingsworth, M. D.; Brown, M. E.; Santarsiero, B. D.; Huffman, J. C.; Goss, C. R. *Chem. Mater.* **1994**, *6*, 1227
(19) Hollingsworth, M. D.; Santarsiero, B. D.; Oumar-Mahamat, H.; Nichols, C. J. *Chem. Mater.* **1991**, *3*, 23.
(20) Leiserowitz, et al. have demonstrated that it is possible to modify the morphologies of hydrogen-bonded crystals by selectivity inhibiting the rate of growth along a given face of a crystal: Addadi, L.; Berkovitch-Yellin, A.; Weissbuch, I.; Mil, J. V.; Shimon, L. J. W.; Lahav, M.; Leiserowitz, L. *Angew. Chem., Int. Ed. Engl.* **1985**, *33*, 466.
(21) (a) Lehn, J. M. *Angew. Chem., Int. Ed. Eng.* **1990**, *29*, 1304. (b) Lehn, J.-M.; Mascal, M.; DeCian, A.; Fischer, J. *J. Chem. Soc., Perkin Trans. 2* **1992**, 461.
(22) Hosseini, M. W.; Ruppert, T.; Schaeffer, P.; Decian, A.; Kyritsakas, N.; Fischer, J. *J. Chem. Soc., Chem. Commun.* **1994**, 2135.
(23) Fan, E.; Yang, J.; Geib, S. J.; Stoner, T. C.; Hopkins, M. D.; Hamilton, A. D. *J. Chem. Soc., Chem. Commun.* **1995**, 1251.

S0002-7863(95)02836-8 CCC: $12.00 

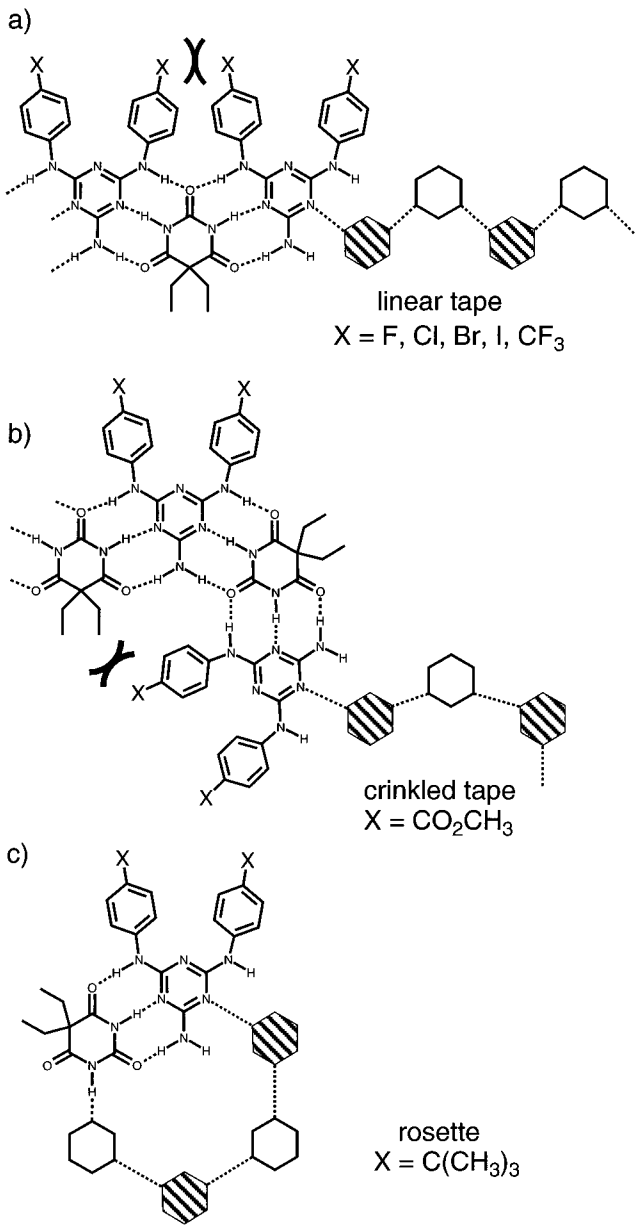


**Figure 1.** Interactions between neighboring phenyl groups in a developing linear tape (a) can force adoption of a crinkled tape (b); further steric stresses, now with barbituric acid substituents, lead to the rosette (c).

solid form) also complicated the comparison of crystalline structures in this series. We detected polymorphism in two cases (X = Br and $CF_3$). To predict crystal structure on the basis of molecular structure, each perturbation of molecular structure should lead to only one type of crystal structure. We hypothesized that polymorphism resulted from conformational isomerism around the phenyl−nitrogen bond. Since many torsions of the phenyl rings were possible, there was no well-defined minimum of free energy in the crystal. Obtaining single crystals was an additional problem in this series because growth along the long axis of the tape was fast relative to growth in other directions; thus, the cocrystals were usually very fine needles.

To avoid the problems associated with the (Bar·Mel$(PhX)_2$) series, we searched for systems that could form only one tape motif and had no possibility for conformational polymorphism. We identified derivatives of 2-benzimidazolone as a class of molecules with potential to form linear tapes in the solid state.[24] Unlike the (Bar·Mel$(PhX)_2$) system, there is only one orientation of the hydrogen-bond donor/acceptor pair that permits tapes in

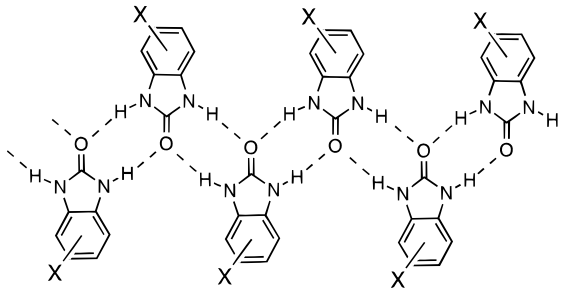

**Figure 2.** Tapes of substituted derivatives of 2-benzimidazolones.

2-benzimidazolones (Figure 2). The benzimidazolones are rigid, so conformational polymorphism is not possible. Polymorphism based on torsions associated with the substituents can be prevented by choosing only axially symmetrical substituents. We also hypothesized that using a molecule that could form two hydrogen bonds, rather than the three of the (Bar·Mel-$(PhX)_2$) system, would make kinetics of growth along the hydrogen-bond axis less favored. Slower growth along the hydrogen-bond axis might promote three-dimensional crystals rather than the very thin needles observed in the (Bar·Mel-$(PhX)_2$) system.[23]

A primary objective of this work was to identify factors that influence the packing of tapes of benzimidazolones in the solid state. Ideally, the tapes will pack in the crystal with a minimum of free energy. Molecules have to be close together for favorable interactions to occur, but they must not be so close that unfavorable interactions overwhelm the favorable ones. Kitaigorodskii described the ideal packing as one in which "no molecules are suspended in empty space and none overlap."[25] This relationship of lowest free energy to closest packing suggests that tapes should leave as little empty volume in the crystal as possible. Thus, we hoped that we might be able to predict the packing arrangement on the basis of closest packing of tapes.

Since tapes of benzimidazolones are planar, substitution of the aromatic ring primarily affects the profile of the edge of the tape. To fill as much space as possible, tapes with scalloped edges (small substituents) should pack in a nonparallel arrangement, while tapes with smooth edges (large substituents) should pack in a parallel arrangement (Figure 3). We also expected electrostatic interactions between aromatic rings to influence the packing. Desiraju and Gavezzotti have suggested that polynuclear aromatic hydrocarbons adopt orientations that maximize two specific interactions: (i) van der Waals interaction between carbon atoms in the rings (that is, geometries in which the aromatic rings are parallel) or (ii) electrostatic attraction between a hydrogen and carbon in the ring (that is, geometries in which aromatic rings pack at an angle to one another).[26] In some cases, the packing arrangement of an unsubstituted aromatic compound shifts from nonparallel to parallel for a heterocyclic analog. Desiraju and Gavezzotti argue that this shift occurs because there are fewer hydrogen atoms around the rim of the ring in the heterocycle (and hence fewer C−H bonds to interact with the proximate aromatic $\pi$ orbitals) than in the unsubstituted aromatic compound.

The unsubstituted 2-benzimidazolone **1-H$_2$**—the only 2-benzimidazolone that has been previously characterized in the solid state—forms tapes that pack at an angle to one another.[27] This nonparallel packing arrangement is consistent with electrostatic interactions between a hydrogen atom of an aromatic C−H bond

(24) MacDonald, J. C.; Whitesides, G. M. *Chem. Rev.* **1994**, *94*, 2303.

(25) Kitaigorodskii, A. I. *Molecular Crystals and Molecules*; Academic Press: New York, 1973.

(26) Desiraju, G. R.; Gavezzotti, A. *J. Chem. Soc., Chem. Commun.* **1989**, 621.

(27) Herbstein, F. H.; Kapon, M. *Z. Kristallogr.* **1985**, *173*, 249.

**Table 1.** Crystallographic Data for Compounds **1** and **2**

| urea | class | space group | *a* (Å) | *b* (Å) | *c* (Å) | *b* (deg)[a] | $R_1$[b] | $R_2$[c] | density (g/cm$^3$)[d] | solvent[e] | crystal shape | melting point (°C) | $C_k$*[f] |
|---|---|---|---|---|---|---|---|---|---|---|---|---|---|
| **1-(CH$_3$)$_2$** | II | $P2_1/c$ | 8.0616(9) | 7.186(1) | 13.9442(9) | 96.300(7) | 0.048 | 0.223 | 1.34 | DMF | blocks | 395 | 0.71 |
| **1-Cl$_2$** | II | $P2_1/c$ | 7.800(2) | 7.193(4) | 13.723(3) | 92.94(2) | 0.055 | 0.191 | 1.75 | DMF | blocks | 398 | 0.71 |
| **1-Br$_2$** | II | $P2_1/a$ | 14.051(6) | 7.267(2) | 7.967(4) | 93.38(4) | 0.099 | 0.316 | 2.39 | CH$_3$OH | blocks | 386 (dec) | 0.72 |
| **1-H$_2$** | × | $P2_1/n$ | 5.296 | 5.738 | 23.440 | 94.50 | 0.052 | | 1.42 | CH$_3$OH | blocks | 316[g] | 0.70 |
| **2-H$_2$** | × | $P2_1/n$ | 6.0397(8) | 4.0704(9) | 34.706(5) | 90.90(1) | 0.051 | 0.220 | 1.43 | CH$_3$OH | blades | 394 | 0.72 |
| **1-F$_2$** | **3-D** | $P2_1/c$ | 8.2319(6) | 7.3405(4) | 11.3087(5) | 90.530(5) | 0.034 | 0.099 | 1.65 | THF/Et$_2$O | plates | 332 | 0.69 |
| **1-I$_2$** | **3-D** | $P2_1/a$ | 14.156(6) | 4.780(6) | 14.391(3) | 108.19(2) | 0.045 | 0.124 | 2.77 | CH$_3$OH | plates | 377 (dec) | 0.68 |

[a] $\alpha$ and $\gamma$ are constrained to be 90° by the symmetry of the space group. [b] This value is the crystallographic Reliability Index, $R_1 = \sum|F_o - F_c|/\sum F_o$ for $F_o > 2\sigma$. [c] $R_2 = \sum|F_o^2 - F_c^2|/\sum F_o^2$ for all $\sigma$. [d] Calculated using the program Cerius2.[34] [e] Solvent used for the growth of single crystals for X-ray crystallograhy. [f] $C_k$* is the packing fraction: $C_k^* = N(V_m/V_c)$, where $N$ is the number of molecules in the unit cell, $V_m$ is the volume of the molecules in the unit cell (calculated with the program Platon[35] rather than using tables of incremental volumes, as done by Kitiagorodski),[25] and $V_c$ is the total volume of the unit cell. [g] Lit.[36] 309−310 °C.

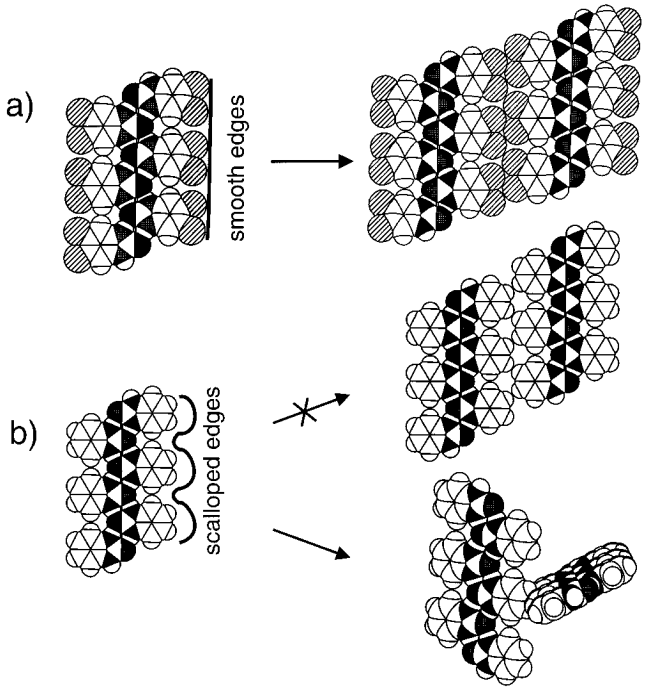


**Figure 3.** Schematic showing the packing arrangements for hydrogen-bonded tapes. (a) Tapes with substituents larger than hydrogen have "smooth" edges. These tapes pack with their long axes parallel and form sheets that are infinite in two dimensions. (b) Tapes substituted only with hydrogen have "scalloped" edges and pack with their long axes at an angle to one another. This arrangement fills the hollows of the scalloped edges (bottom) and increases the filling of space. The parallel packing arrangement leaves empty space between adjacent tapes.

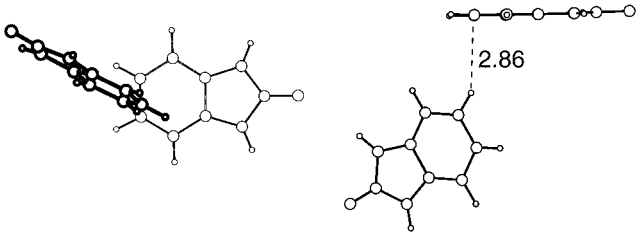


**Figure 4.** Close contact (2.86 Å) between a hydrogen on one aromatic ring and a carbon on an adjacent aromatic ring in 2-benzimidazolone (**1-H$_2$**). This contact is 0.04 Å shorter than the sum of the van der Waals radii.

on one molecule and a carbon atom in the ring of a neighboring molecule (Figure 4). It is also the arrangement we would expect on the basis of the scalloped edges. This analysis of the packing as a combination of closest packing and local electrostatic interactions suggested a strategy for manipulating crystal structure by perturbing molecular structure: substitution in the 4 and 5 positions of the aromatic ring with atoms larger than hydrogen would provide smooth "edges" along the tape and promote parallel packing.

**Scheme 1.** Synthesis of the Benzimidazolones **1-X$_2$** and **2-H$_2$**

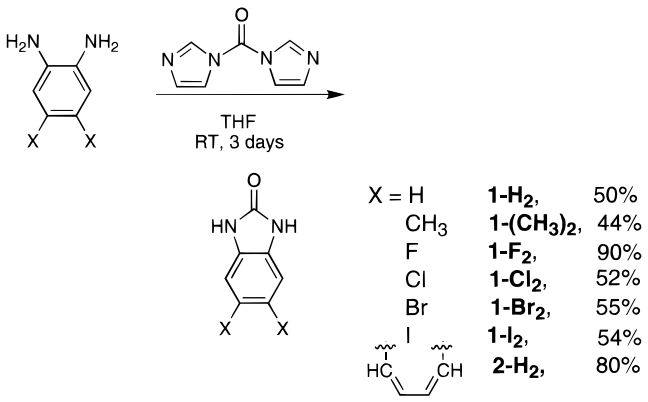


In this work, we investigated a series of 4,5-disubstituted derivatives of 2-benzimidazolone to determine how substituents on the aromatic ring influenced the formation and packing of tapes. We demonstrate that substituents in these positions direct both the hydrogen-bonding motif adopted in the solid state and the packing arrangement of hydrogen-bonded tapes. To minimize free volume in a crystal and maximize interactions between aromatic carbons and hydrogens, tapes with scalloped edges pack in a nonparallel arrangement. Tapes with smooth edges and few aromatic hydrogens pack in a parallel arrangement. The presence of weak electrostatic interactions between substituents on the 2-benzimidazolones can shift the hydrogen-bond pattern from a tape motif to a three-dimensional network motif. These results provide a basis for prediction of the structure of other derivatives of benzimidazolones in the solid state.

## Results and Discussion

**Synthesis and Crystallization of 4,5-Disubstituted Benzimidazolones.** We prepared a series of benzimidazolones by the reaction of the appropriate derivative of *o*-phenylenediamine with 1,1′-carbonyldiimidazole (Scheme 1). Compound **1-H$_2$** has been previously synthesized by several alternative routes.[28−32] The best solvents for crystallizing **1-H$_2$**, **1-(CH$_3$)$_2$**, **1-Cl$_2$**, **1-Br$_2$**, **1-I$_2$**, and **2-H$_2$** were polar protic and aprotic solvents: hot methanol, warm dimethylformamide, pyridine, and *N*-meth-

(28) Agrawal, V. K.; Sharma, S. *Indian J. Chem., Sect. B* **1982**, *21B*, 967.
(29) Almeida, P. S.; Lobo, A. M.; Prabhakar, S. *Heterocycles* **1989**, *28*, 653.
(30) Crotti, C.; Cenini, S.; Ragaini, F.; Porta, F.; Tollari, S. *J. Mol. Catal.* **1992**, *72*, 283.
(31) Heyman, D. A. *J. Heterocycl. Chem.* **1978**, *15*, 573.
(32) Yoshida, T.; Kambe, N.; Murai, S.; Sonoda, N. *Bull. Chem. Soc. Jpn.* **1987**, *60*, 1793.

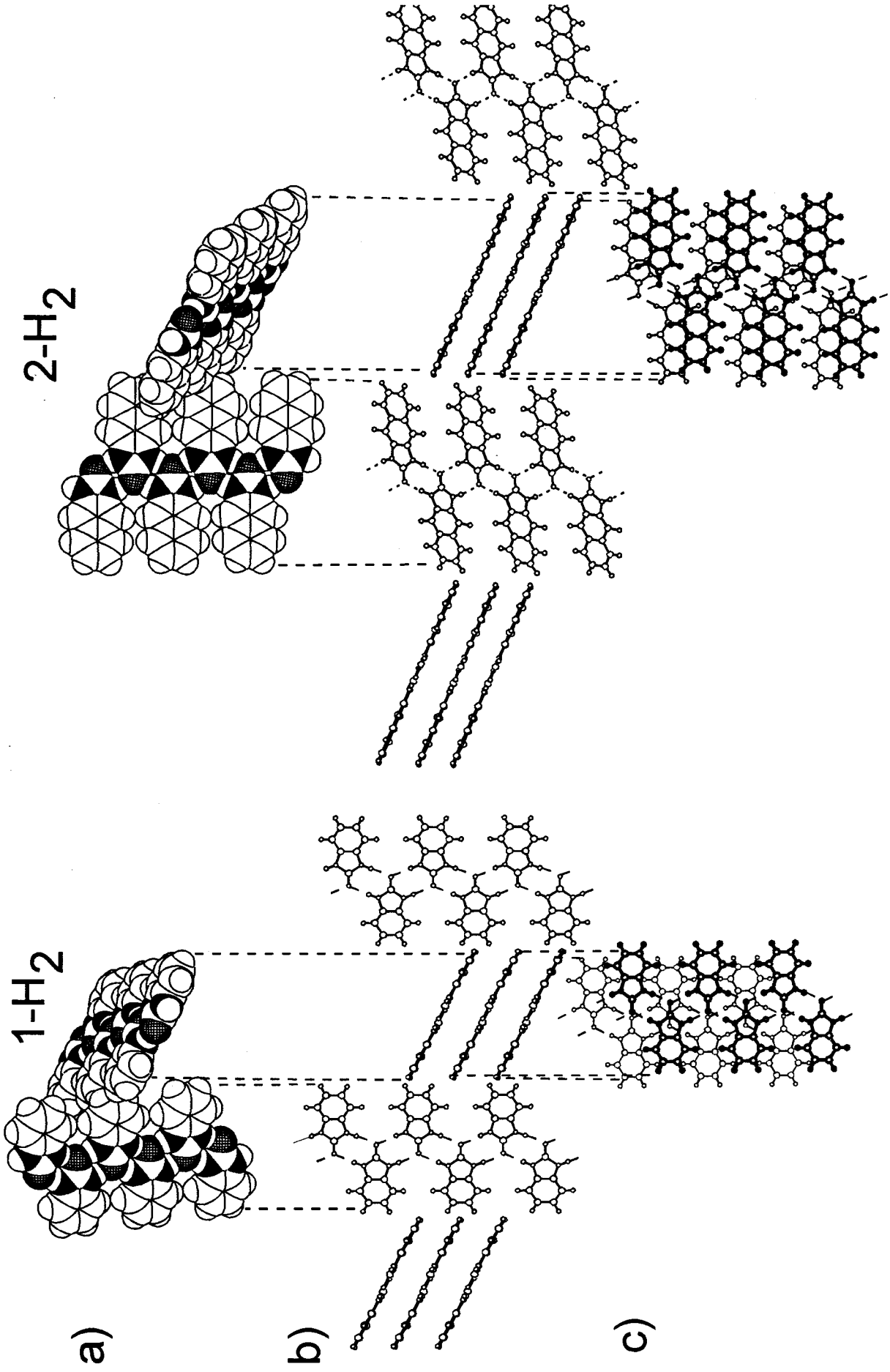


**Figure 5.** Three views of the packing arrangement for **1-H$_2$** and **2-H$_2$**: (a) a space-filling model of adjacent tapes, (b) a view looking down the long axis of the horizontal tapes, and (c) a top-down view showing the position of one tape (dark) with respect to tape in the layer directly below (light). The planar tapes of **1-H$_2$** and **2-H$_2$** stacked on top of one another in a stair-step arrangement, with each tape shifted along both the long and short axes with respect to the tape below.

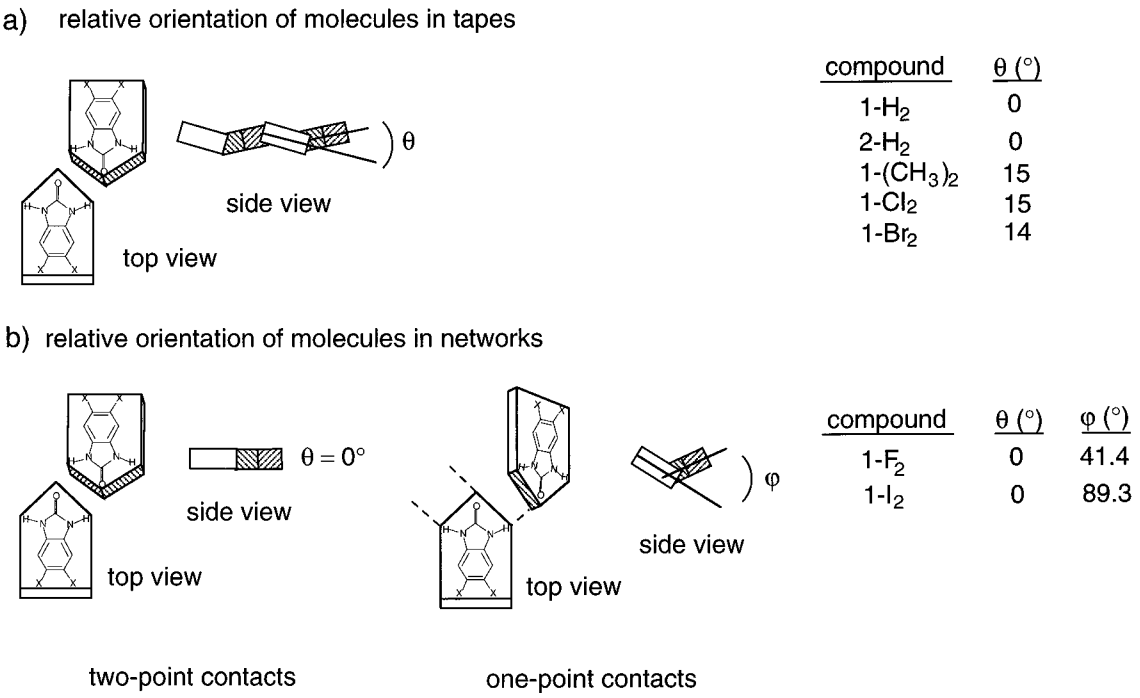


| compound | θ (°) |
|---|---|
| 1-$H_2$ | 0 |
| 2-$H_2$ | 0 |
| 1-$(CH_3)_2$ | 15 |
| 1-$Cl_2$ | 15 |
| 1-$Br_2$ | 14 |

| compound | θ (°) | φ (°) |
|---|---|---|
| 1-$F_2$ | 0 | 41.4 |
| 1-$I_2$ | 0 | 89.3 |

**Figure 6.** Orientations of molecules: (a) $\theta$ is the dihedral angle between the planes of opposing molecules in the tape. Tapes of **1-H₂** and **2-H₂** are planar ($\theta = 0°$). Tapes of **1-(CH₃)₂**, **1-Cl₂**, and **1-Br₂** are "buckled" ($\theta < 0°$). (b) $\theta$ is the dihedral angle between the planes of opposing molecules joined by a two-point contact. $\varphi$ is the dihedral angle between the planes of opposing molecules joined by a one-point contact.

ylpyrolidinone. The initial dissolution of the compounds usually required a large amount of hot solvent (1−3 L/g of solute). Subsequent evaporation of low-boiling solvents such as methanol under ambient conditions yielded single crystals as needles, blocks, or plates. For higher boiling solvents, slow cooling of the solutions, sometimes after dilution with diethyl ether, gave the best quality crystals. The presence of solvents with good hydrogen acceptor and donor sites did not interfere with formation of the tapes: none of the crystals incorporated molecules of solvent into their lattice. The solubility of **1-H₂**, **1-(CH₃)₂**, **1-Cl₂**, **1-Br₂**, **1-I₂**, and **2-H₂** in polar solvents such as THF, $CH_2Cl_2$, acetone, and water was negligible. In contrast, **1-F₂** was soluble in THF, $CH_2Cl_2$, and acetone was crystallized from concentrated solutions of these solvents upon dilution of diethyl ether by vapor diffusion at room temperature, and gave thick rectangular or hexagonal plates. Compound **1-F₂** also crystallized from mixtures of THF or acetone with water upon slow evaporation of the organic solvent.

**Characterization of the Structures of 4,5-Benzimidazolones in the Solid State.** We solved the crystal structures of **1-(CH₃)₂**, **1-Cl₂**, **1-Br₂**, **2-H₂**, **1-F₂**, and **1-I₂** (Table 1) to evaluate patterns of hydrogen bonds and packing arrangements. The crystal structure of **1**-$H_2$ has been reported,[27] and we have included the data for comparison with the substituted benzimidazolones. All the crystals were monoclinic and members of the centric family of $P2_1$ space groups. Their packing fractions, ($C_k$*,[33] Table 1) fell in the narrow range of 68−72%, typical for organic compounds.[25] Most of the 2-benzimidazolones formed tapes, but there were also instances of a three-dimensional network of hydrogen bonds (**3-D**). The tapes packed in two different arrangements, parallel (||) and nonparallel (×). We discuss the structures in the sections that follow.

**1-H₂ and 2-H₂ Form Tapes That Pack in with Their Long Axes Nonparallel (×).** Like tapes of **1-H₂**, tapes of **2-H₂** have scalloped edges; thus, we predicted that tapes of **2-H₂** would pack in a nonparallel arrangement to fill the empty spaces at the edges of the tape. The structure of **2-H₂** was indeed closely related to the known structure of **1-H₂** (Figure 5). The tapes of both compounds were planar (Figure 6), the hydrogen bonds had similar lengths, and the hydrogen-bond angles were nearly linear (Table 2). In both compounds, the tapes stacked with the aromatic rings in one tape offset from those of the tapes above and below, presumably to minimize repulsion between $\pi$-systems.[37−39] The stacks of tapes packed at an angle to one another with molecules from one tape occupying some of the space between molecules in an adjacent tape.

The relative orientations of molecules in adjacent stacks of **2-H₂** were different than in those in adjacent stacks of **1-H₂** (Figure 5a). We did not identify specific interactions responsible for the difference in relative orientations; the orientations might be dictated purely by closest packing. In both **1-H₂** and **2-H₂**, there were interactions between an aromatic hydrogen and an aromatic carbon (C···H). The C···H contact in **1-H₂** was a short contact (slightly less than the sum of the van der Waals radii)[41] and thus suggested an electrostatic attraction between carbon and hydrogen (Table 3). The C···H contact in **2-H₂** was longer than that in **1-H₂** (Table 3). This lengthening suggested that the C···H interaction was less important in the **2-H₂** than in **1-H₂**. These data are consistent with the hypothesis that closest packing is the most important determinant of the packing for benzimidazolones with only hydrocarbon substituents.

(33) We have calculated the packing fractions ($C_k$*) using molecular volume with the program Platon (see ref 35). The packing fraction ($C_k$) is traditionally calculated using tables of average volume increments. We prefer the former approach because some functional groups do not have tabulated values and because molecular volumes depend on the environment.

(34) Cerius2 1.0 molecular modeling program, MSI: Burlington, MA, 1994.
(35) Pluton-92 (Version 28) and Platon-92 (Version 25): A. L. Spek, Bijvoet Center for Biomolecular Research, Vakgroep Kristal- en Structurechemie, University of Utrecht.
(36) Hershenson, F. M.; Bauer, L.; King, K. F. *J. Org. Chem.* **1968**, *33*, 2543.
(37) Hunter, C. A.; Sanders, J. K. M. *J. Am. Chem. Soc.* **1990**, *112*, 5525.
(38) Cozzi, F.; Cinquini, M.; Annunziata, R.; Dwyer, T.; Siegel, J. S. *J. Am. Chem. Soc.* **1992**, *114*, 5729.
(39) Cozzi, F.; Cinquini, M.; Annuziata, R.; Siegel, J. S. *J. Am. Chem. Soc.* **1993**, *115*, 5330.
(40) Taylor, R.; Kennard, O. *Acc. Chem. Res.* **1984**, *17*, 320.
(41) We used the van der Waals radii given by Bondi (Å): 1.47 (F), 1.75 (Cl), 1.85 (Br), 1.98 (I). See: Bondi, A. *J. Phys. Chem.* **1964**, *68*, 441.

**Table 2.** Summary of Hydrogen-Bond Distances and Angles

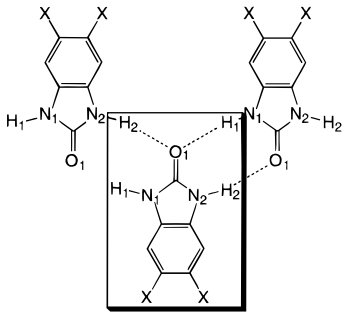

| | class | **O(1)**···N(1)[a] (Å) | **O(1)**···N(2)[a] (Å) | angle (deg)[b] **O(1)**···H(1)···N(1) | angle (deg)[b] N(2)···H(2)···**O(1)** | angle (deg)[c] H(2)···**O(1)**···H(1) |
|---|---|---|---|---|---|---|
| **1-H$_2$** | × | 2.84 | 2.84 | 176.2 | 176.2 | 127.5 |
| **2-H$_2$** | × | 2.84 | 2.80 | 167.4 | 174.1 | 124.1 |
| **1-(CH$_3$)$_2$** | ‖ | 2.79 | 2.86 | 167.7 | 167.2 | 118.2 |
| **1-Cl$_2$** | ‖ | 2.78 | 2.85 | 171.8 | 170.9 | 126.7 |
| **1-Br$_2$** | ‖ | 2.87 | 2.79 | 140.8 | 156.4 | 117.2 |
| **1-F$_2$** | **3-D** | 2.89 | 2.82 | 163.1 | 161.5 | 91.2 |
| **1-I$_2$** | **3-D** | 2.85 | 2.85 | 164.2 | 161.8 | 124.1 |

[a] The atom in bold belongs to the central molecule highlighted with the box. The atoms in plain text belong to the adjacent molecules. We give only the distance between the N and O atoms on adjacent hydrogen-bonded molecules, which we believe is subject to less error than distances involving the hydrogen atoms. The positions of the hydrogen atoms were fixed at idealized positions in some structures and refined in others, introducing variability in distances. [b] These values are the angles of three atoms involved in one hydrogen bond. The mean value for amides is 161.2°.[40] [c] These values are the angles between the amide N-H, the carbonyl oxygen, and a second amide N-H.

**1-(CH$_3$)$_2$, 1-Cl$_2$, and 1-Br$_2$ Form Tapes That Pack with Their Long Axes Parallel (‖).** The crystal structures of **1-(CH$_3$)$_2$**, **1-Cl$_2$**, and**1-Br$_2$** were effectively isostructural (Figure 7). The hydrogen bonds were essentially the same length for all three tapes (2.78−2.89 Å) (Table 2).[42] Unlike the × tapes, these ‖ tapes were not completely planar: the tapes buckled so that opposing hydrogen-bonded molecules within a tape lay at an angle to one another ($\theta$, Figure 6). The buckling may alleviate steric interaction between substituents on adjacent molecules on the same side of the tape or, perhaps, unfavorable steric interaction between tapes in adjacent layers.[43]

Tapes composed of **1-(CH$_3$)$_2$**, **1-Cl$_2$**, and **1-Br$_2$** packed with their long axes *parallel*, in sheets that were infinite in two dimensions (Figure 7a). The substituents on the edges of one tape packed in between the substituents on an adjacent tape. The substituents packed particularly closely in **1-Cl$_2$** and **1-Br$_2$**, where the distances between halogen atoms in adjacent tapes are slightly shorter than the sum of the isotropic van der Waals (VDW) radii (Table 3).[41,44−46] The sheets stacked on top of one another (Figure 7b). Compared with × tapes, the ‖ tapes were offset significantly along their short axes relative to the tapes above and below (Figure 7c). This offset presumably prevents unfavorable steric interaction between substituents on molecules in one layer with substituents on molecules in the layers above and below. The offset suggests another reason why benzimidazolones with substituents other than hydrogen

(42) The *R* factor for **1**-Br$_2$ is high because the crystals were twinned. The errors in distances associated with **1**-Br$_2$ are expected to be higher than distances for the other compounds in Table 2.

(43) We observed a similar buckling in the rosette (cyclic hexamer) structures in the (Bar·Mel(PhX)$_2$) system. Modeling of this system also indicated that buckling was not a steric requirement for the motif itself, and we believe that buckling occurs only within the crystal.

(44) Short contacts between chlorines or between bromines in halogenated aromatics have been reported in many instances and are apparently the primary influence on crystal structure in some cases (see refs 45 and 46) In the present series, the fact that the methyl-substituted cyclic urea adopts the same structural motif as the chloro- and bromo-substituted benzimidazolones suggests that chlorine−chlorine and bromine−bromine interactions do not influence the packing of parallel tapes.

(45) Desiraju, G. R.; Sarma, J. A. R. P. *Proc. Indian Acad. Sci. Chem. Sci.* **1986**, *96*, 599.

(46) Desiraju, G. R.; Parthasarathy, R. *J. Am. Chem. Soc.* **1989**, *111*, 8725.

**Table 3.** Summary of Selected Intermolecular Close Contact Distances between the Asymmetric Molecule and Its Neighbors

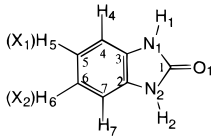

| | distance (Å)[a] | ± sum of VDW | atom *i*···atom *j*[b] | note[c] | electrostatic[d] | VDW |
|---|---|---|---|---|---|---|
| **1-H$_2$** | *2.86* | *−0.04* | *C(6)···H(6)* | < | · | |
| | *2.86* | *−0.04* | *H(6)···C(6)* | < | · | |
| | 3.07 | 0.17 | C(6)···H(5) | | | |
| | 3.09 | 0.19 | C(5)···H(6) | | | |
| | 3.09 | 0.19 | H(6)···C(5) | | | |
| | 3.07 | 0.17 | H(5)···C(6) | | | |
| **2-H$_2$** | *2.95* | *0.05* | *C(8)···H(8)* | | · | |
| | 2.95 | 0.05 | H(8)···C(8) | | · | |
| **1-F$_2$**[e] | *2.53* | *−0.14* | *F(1)···H(4)* | < | · | |
| | *2.74* | *0.07* | *F(1)···H(7)* | | · | |
| | **2.84** | **−0.10** | **F(2)···F(2)** | < | | · |
| | *2.53* | *−0.14* | *H(4)···F(1)* | < | · | |
| | *2.86* | *0.19* | *H(1)···F(2)* | | · | |
| | *2.74* | *0.07* | *H(7)···F(1)* | | · | |
| **1-Cl$_2$** | **3.43** | **−0.07** | **Cl(2)···Cl(2)** | < | | · |
| | *3.46* | *0.19* | *Cl(2)···O(1)* | | · | |
| | *3.48* | *0.03* | *C(3)···Cl(2)* | | · | |
| | *3.46* | *0.19* | *O(1)···Cl(2)* | | · | |
| **1-Br$_2$** | **3.76** | **0.06** | **Br(1)···Br(1)** | | | · |
| | **3.59** | **−0.11** | **Br(2)···Br(2)** | < | | · |
| | *3.54* | *−0.01* | *C(3)···Br(2)* | < | · | |
| **1-I$_2$**[f] | **3.88** | **−0.09** | **I(1)···I(2)** | < | | · |
| | **3.92** | **−0.04** | **I(1)···I(1)** | < | | · |
| | **4.07** | **0.11** | **I(1)···I(2)** | | | · |
| | **3.88** | **−0.09** | **I(2)···I(1)** | < | | · |
| | **4.07** | **0.11** | **I(2)···I(1)** | | | · |

[a] Atoms in bold involve halogen−halogen contacts; atoms in italics are other halogen−non-halogen contacts and close contacts between aromatic rings. [b] Atom *i* is an atom from the asymmetric molecule. Atom *j* is an atom from a neighboring molecule. [c] Symbols: < denotes contacts less than the sum of the van der Waals radii. These calculations used values of the radii from Bondi (Å): 1.47 (F), 1.75 (Cl), 1.85 (Br), 1.98 (I). [d] The partial charges were derived from semiempirical calculations (ESP charges using MOPAC6.0) as described in the text. [e] The asymmetric molecule of **1-F$_2$** and its nearest neighbors are shown in Figure 12. [f] The asymmetric molecule of **1-I$_2$** and its nearest neighbors are shown in Figure 13.

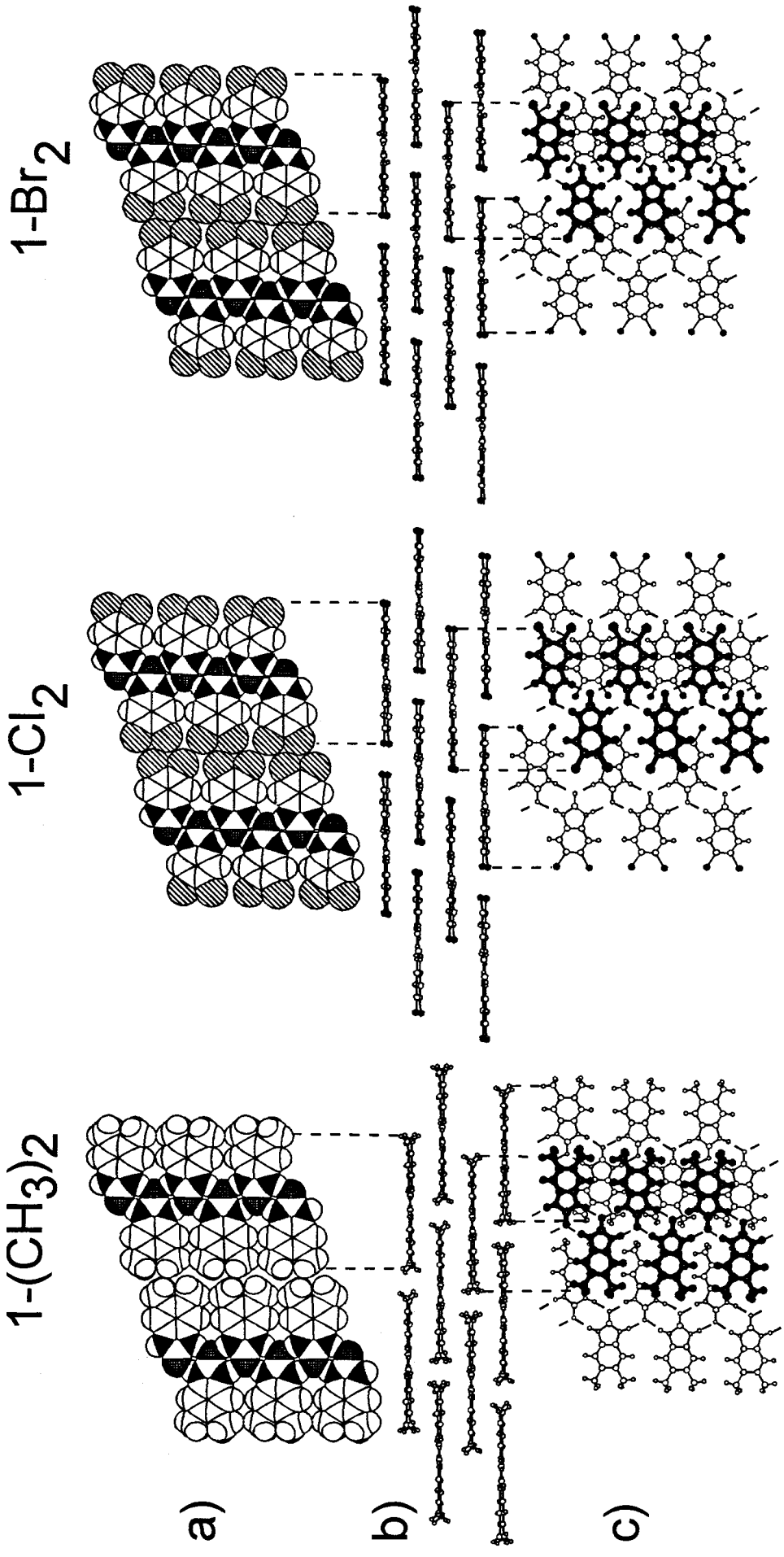


**Figure 7.** Three views of the packing arrangement for compounds **1-(CH$_3$)$_2$**, **1-Cl$_2$**, and **1-Br$_2$**: (a) a space-filling model looking down on a layer composed of tapes, (b) an end-on view looking down the long axis of the tape, and (c) a second top-down view showing the position of one tape (dark) with respect to tapes in the layer below (light).

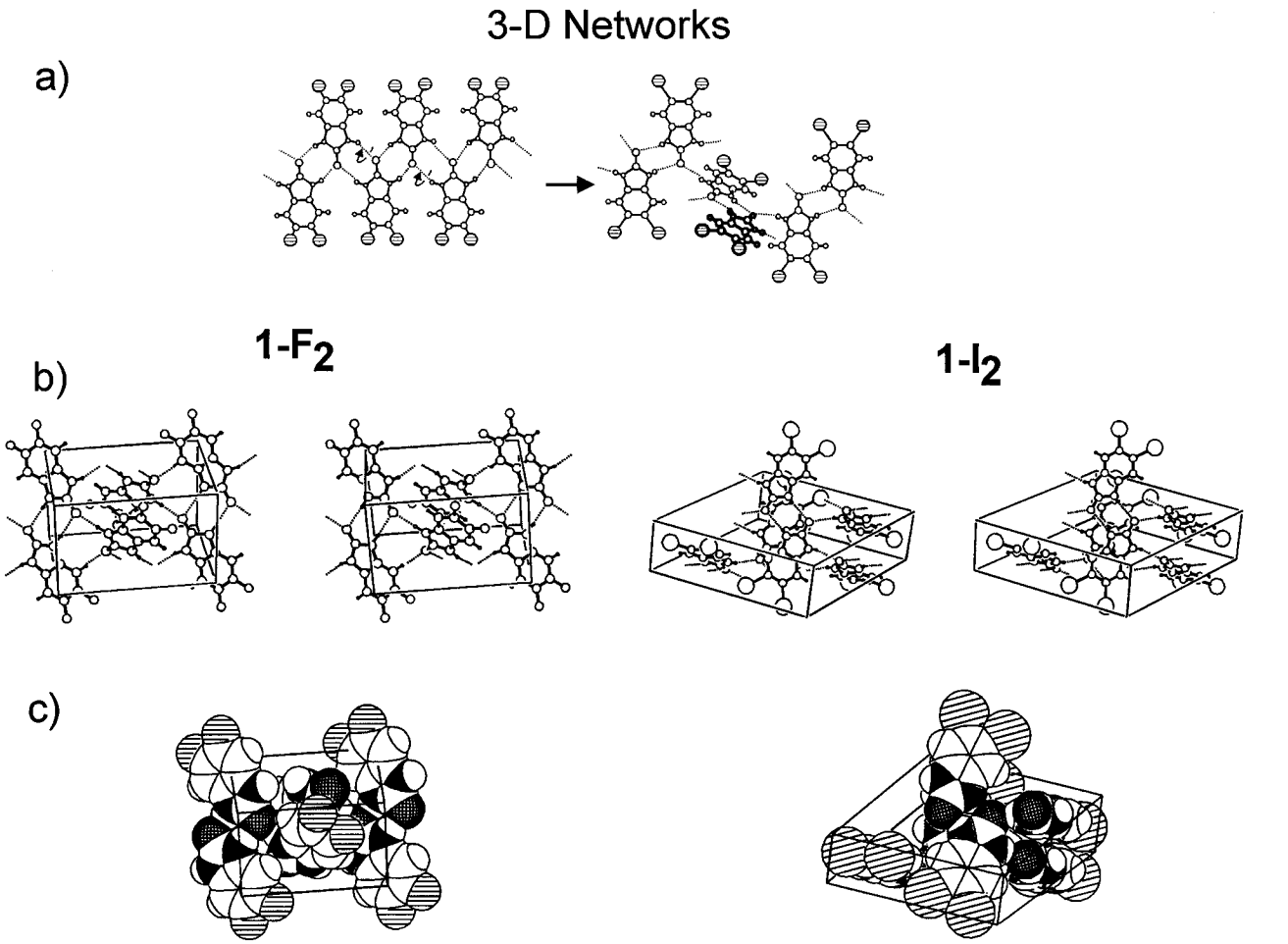


**Figure 8.** Three views of the packing arrangement for each compound: (a) a simplified schematic showing the relationship of the tape motif to the network motif, (b) a stereoview of the network, emphasizing the three-dimensional nature of the connectivity of hydrogen bonds, and (c) a space-filling model of a portion of the network.

cannot form × tapes: tapes of these compounds cannot stack directly on top of one another to form the stacks observed for **1-H$_2$** and **2-H$_2$**.

**Benzimidazolones 1-F$_2$ and 1-I$_2$ Form a Network (3-D) Motif, Rather Than a Tape Motif.** In the network motif, each molecule is hydrogen-bonded through a two-point contact (cyclic dimer) to one molecule and through one-point contacts to two other molecules (Figure 8). These networks may be viewed as "broken tapes," in which every other set of hydrogen bonds is broken and rejoined to two different molecules outside the plane of the tape (Figure 8a). The hydrogen bonds in **1-F$_2$** and **1-I$_2$** were similar in length to the hydrogen bonds in both parallel and nonparallel tapes (Table 2). The molecules involved in the two-point contact (dimers) were coplanar ($\theta = 0°$) while the molecules involved in the one-point contact lay at angle to one another ($\varphi$, Figure 6).

**Infrared Spectroscopy Suggests That the Energy of the Hydrogen Bonds Is Comparable in Tape and 3-D Motifs.** We expected the energy of the hydrogen bonds to be similar for compounds **1-X$_2$** and **2-H$_2$**: the number of hydrogen bonds is conserved in each structural type, and the lengths and angles of the hydrogen bonds are similar for all the compounds studied (Table 2). We further analyzed the strengths of the hydrogen bonds by infrared spectroscopy (Nujol mulls of crystalline samples) (Figure 9). The carbonyl stretch has been used as an indicator of the strength of hydrogen bonds: stronger hydrogen bonds shift the stretch to lower energy.[47] By the criterion of the carbonyl stretch, hydrogen bonds in the **3-D** motif are stronger than those in the × tapes but comparable to those in the || tapes. Thus, tapes are not necessarily constituted of stronger hydrogen bonds than are the **3-D** motifs.

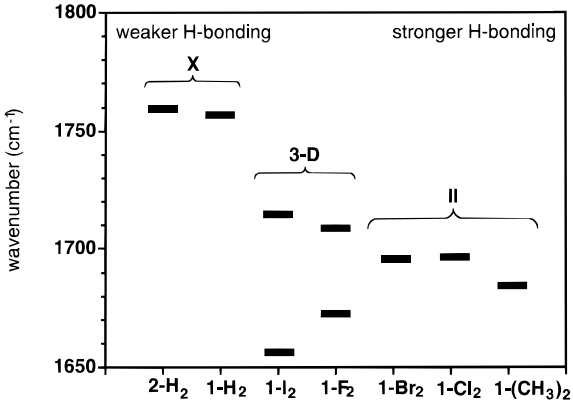


**Figure 9.** Energies of the carbonyl stretches in the infrared spectra of **1-X$_2$** and **2-H$_2$**. Compounds that crystallize in the 3-D network have two carbonyl stretches because the environment of the carbonyl is unsymmetrical—a two-point contact on one side and two one-point contacts on the other. The energies of the carbonyl stretches of compounds bearing electron-withdrawing substituents are similar to the energy of a compound bearing an electron-donating substituent (**1-(CH$_3$)$_2$**). This similarity indicates that the influence of the substituent on the energy of the carbonyl stretch is small compared to the influence of structural type.

**Comparison of the Calculated Lattice Energies Also Indicates That Energies of Hydrogen Bonds Are Similar in Both the Tape and 3-D Motifs.** Analyzing the components of the lattice energy ($U_{latt}$) of the crystals using computations is an alternative way of comparing the strengths of the hydrogen

(47) Susi, H. *Methods Enzymol.* **1972**, *26*, 381.

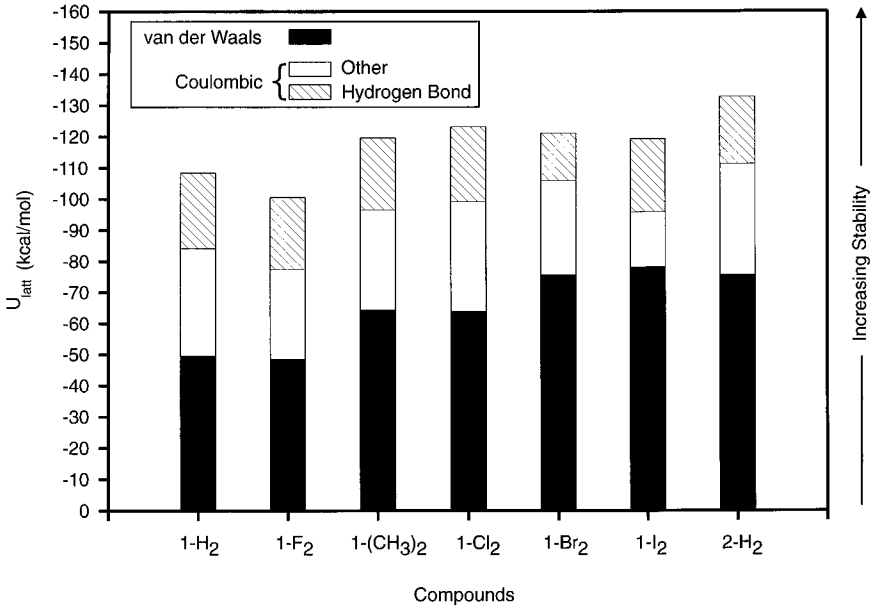


**Figure 10.** Calculated lattice energies ($U_{latt}$) for the benzimidazolones, including the van der Waals and Coulombic components. The portion of the Coulombic term that results from hydrogen bonds is marked with hatches.

bonds in the crystals. In these calculations, the coordinates of each molecule from the single crystal data served as the starting point. The geometry of a single molecule was first optimized until the gradient in its energy was below 0.01 kcal/mol using the semiempirical AM1 Hamiltonian in MOPAC6,[48] electrostatic potential (ESP) partial charges were assigned,[49] and this final geometry was used for further computations. To determine $U_{latt}$, we used the Cerius2 modeling program[34] and the Drieding force field (with the ESP charges from MOPAC6.0).[50] The van der Waals interactions were truncated at 8 Å, and the Ewald summation technique was used for Coulombic interactions in the crystal.[51,52] The appropriate crystalline system for each molecule was built in Cerius2, and the energy of the crystal was minimized until the gradient in energy was below 0.01 kcal/mol. The values of $U_{latt}$ were calculated from this minimized system, and the contributions from van der Waals and electrostatics analyzed (Figure 10). The results of $U_{latt}$ suggest that the contribution from the hydrogen bonds—a component of the electrostatics—is similar for all the molecules regardless of the motif. These data from computations, and those from infrared spectroscopy, suggest that the preference of a given molecule for a particular motif is based on interactions involving substituents, rather than strengths of hydrogen bonds.

**Computations Suggest That Tapes of 1-$F_2$ and 1-$I_2$ Are Not Disfavored Outside the Crystalline Environment.** We originally speculated that the failure of **1-$F_2$** and **1-$I_2$** to form tapes was due to unfavorable interactions *within* the tape. For example, electrostatic interactions between C−F bond dipoles and steric interactions between adjacent iodine atoms in different molecules might both be sufficiently unfavorable that, in principle, they destabilized the tapes. To address the question of stability of the tapes outside the environment of the crystalline lattice, we have carried out molecular mechanics calculations on fragments of tapes. In QUANTA 3.3[53] five molecules of

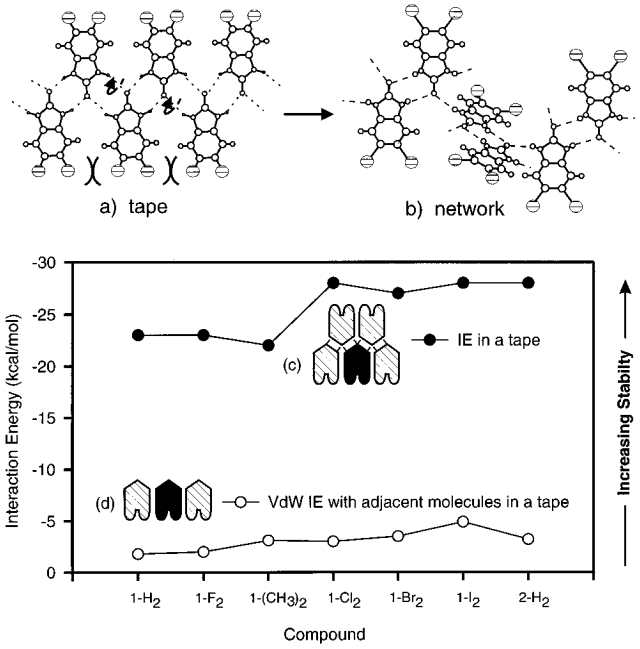


**Figure 11.** Bulky substituents might interact unfavorably in the tape motif and consequently favor the network motif. The graph shows (a) the total interaction energy (IE) between a central cyclic urea (black) and its four closest hydrogen-bonded neighbors (hatched) within a tape and (b) the van der Waals component of the IE between a central cyclic urea and its two adjacent neighbors.

**1-$H_2$** were built and arranged into a tape. The molecules were constrained to be coplanar, with an initial value of 2.8 Å for the N···O═C distance, and the energy of this tape was minimized until its gradient reached 0.01 kcal/mol. Using this energetically minimized tape as a template, we added the various substituents of interest, adjusted the geometries appropriately, and calculated the total interaction energy (IE) of the central cyclic urea with the four neighboring molecules composing the rest of the tape (Figure 11). These IE data showed that a tape of **1-$F_2$** is as favorable as a tape of **1-$H_2$**. Moreover, a tape of **1-$I_2$** is *more* favorable than tapes of any other compound.[54] These data suggest that tapes of **1-$F_2$** and **1-$I_2$** are *not* destabilized relative to other tapes but that these compounds are influenced by interactions outside of a tape motif.

(48) MOPAC6.0: J. J. P. Stewart, QCPE, 455 (V. 6.0). Mopac-ESP: Besler, B. H.; Merz, K. M.; Kollman, P. A. *J. Comput. Chem.* **1990**, *11*, 431.

(49) We calculated the ESP charges using MOPAC6.0: −0.01e (F), +0.16e (Cl), +0.16e (Br), +0.17e (I).

(50) Dreiding II: Mayo, S. L.; Olafson, B. D.; Goddard, W. A. *J. Phys. Chem.* **1990**, *94*, 8897.

(51) Karasawa, N.; Goddard, W. A. *J. Phys. Chem.* **1989**, *93*, 7320.

(52) Ewald, P. P. *Ann. Phys. (Leipzig)* **1921**, *64*, 253.

(53) QUANTA 3.3 molecular modeling program, MSI: Burlington, MA, 1992.

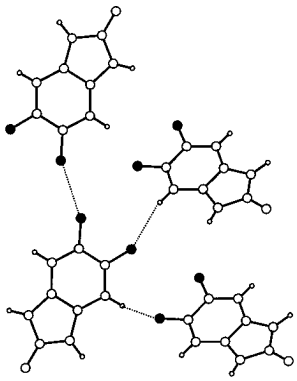

**Figure 12.** asymmetric molecule of **1-F$_2$** with H···F contacts. The fluorine atoms are shaded.

**The Selectivity for the 3-D Motif over That of the Tape Motif in 1-F$_2$ and 1-I$_2$ Seems To Be Due to Interactions Involving the Substituents**. We sought to identify secondary interactions for **1-F$_2$** and **1-I$_2$** that stabilized a **3-D** network relative to a tape. The calculated lattice energies (Figure 10) indicate that Coulombic interactions are more important than van der Waals interactions for molecules with small substituents (**1-H$_2$** and **1-F$_2$**). In contrast, van der Waals interactions are more important than Coulombic interactions for molecules with large substituents (**1-(CH$_3$)$_2$**, **1-Cl$_2$**, **1-Br$_2$**, and **1-I$_2$**). These observations are consistent with a number of analyses of the Cambridge Structural Database.[46,55−58] These analyses indicate that halogens can form short contacts to other halogens and to polar hydrogens. These short contacts have been rationalized in terms of specific intermolecular interactions. Interactions between halogens and polar hydrogens are electrostatic, so the strength of the interaction increases with the ratio of charge to mass (I < Br < Cl < F). The nature of the interactions between two halogens is a subject of debate.[46,59] It is known, however, that the relative order of favorable halogen−halogen interactions is F < Cl < Br < I.[46] The polarizability of iodine, and hence its dispersion energy, is significantly greater than those of the other halogens.[58,60] Therefore, short contacts between iodine atoms should increase the van der Waals interaction contribution to the lattice energy.

**Crystals of 1-F$_2$ Show Short Contacts between Fluorine and Hydrogen Atoms.** Each molecule of **1-F$_2$** forms two short contacts (less than the sum of the VDW radii) between fluorine atoms and aromatic hydrogens (F···H) (Figure 12). None of the other benzimidazolones have short contacts between halogens and aromatic hydrogens. Semiempirical calculations of the partial charges on the atoms in the benzimidazolones suggest that only fluorine is sufficiently electronegative to bear a partial negative charge;[48,49] therefore, only fluorine can interact favorably with an aromatic C−H bond. We propose that the favorable electrostatic interaction between fluorine and hydrogen is a factor that favors the **3-D** motif over the tape for crystals of **1-F$_2$**. We note that the interaction between fluorine and hydrogen need not be very strong, since the preference for the tape motif (if it exists at all) is weak.

**Molecules of 1-I$_2$ Have Five Short Iodine−Iodine Contacts in the 3-D Motif.** Three of these five short contacts (I···I) are less than the sum of the van der Waals radii (Table 3, Figure 13). The **3-D** motif observed for **1-I$_2$** has more short contacts between halogens than does the || tape motif observed for **1-Cl$_2$** and **1-Br$_2$**. The parallel tapes can only form contacts between halogen atoms in the plane of the tape. Halogen−halogen interactions become more important as the polarizability increases: **1-Cl$_2$** has one contact, **1-Br$_2$** has two, and **1-I$_2$** has five (three of which are short contacts). We propose that van der Waals interaction between iodine atoms is sufficiently strong to be an important factor in the selectivity of the motif. The van der Waals interactions between chlorine atoms and bromine atoms are not strong enough to overcome what is otherwise a preference for tapes.

**We Have Not Detected Polymorphism in This Series of Benzimidazolones.** We wished to know whether the observed structures represented a global minimum in free energy for the system or whether there were polymorphs of equal or lower energies. To determine whether polymorphism occurred in this series of benzimidazolones, we examined crystals from each structural class using X-ray powder diffraction (XPD). The XPD pattern provides a fingerprint for a specific crystalline lattice: all powders having the same XPD pattern have identical crystal structures.[61,62] We deliberately attempted to induce the formation of polymorphs by crystallizing selected compounds from each structural class (**1-(CH$_3$)$_2$** (||), **1-H$_2$** (×), and **1-F$_2$** (**3-D**)) from four different solvents. The compounds crystallized upon slow evaporation of the solvent under ambient conditions, diffusion of ether into the solution at room temperature, or rapid cooling of the solution. We obtained crystals of varying size and shape depending on the conditions of crystallization; XPD showed, however, that the structures of these crystals were the same.

For all compounds, the agreement between the *position* of the peaks in the experimental traces and the calculated trace was good and indicated that only one solid phase crystallized under a variety of conditions.[63] For **1-(CH$_3$)$_2$**, the relative *intensities* of the calculated and measured peaks varied considerably for peaks corresponding to certain *hkl* planes. This variation in relative intensity of the peaks suggests that a preferred orientation may occur in the crystalline sample used for XPD.[64]

We were unable to induce a change of phase in the benzimidazolones upon heating. A powdered sample of a member of each class (**1-H$_2$**, **1-F$_2$**, and **1-(CH$_3$)$_2$**) was heated in an open glass vial for 3 days at 160 °C. During this time, some crystals grew on the sides of the vial in the samples of **1-F$_2$** and **1-H$_2$** as a result of sublimation, but the sample of **1-(CH$_3$)$_2$** remained unchanged. After cooling, the samples were reground and the XPD pattern recorded again: the XPD patterns remained unchanged. The XPD pattern of these three molecules did not change for samples grown by sublimation (150 °C, $10^{-3}$ Torr). The absence of polymorphism in this series of benzimidazolones under the conditions we have tested suggests that these

(54) The assertion that **1-I$_2$** is not too large laterally to allow the formation of a tape is further supported by the following observation: the distance between bromine atoms on the same side of a tape of **1-Br$_2$** is 4.0 Å. The I−I contacts in the observed network structure are shorter (3.98 Å) than the 4.0 Å required, so replacing the bromine atoms in **1-Br$_2$** with iodine atoms is not precluded by unfavorable steric interactions.

(55) Kumar, V. A.; Begum, N. S.; Venkatesan, K. *J. Chem. Soc., Perkin Trans. 2* **1993**, 463.

(56) Murray-Rust, P.; Motherwell, W. D. S. *J. Am. Chem. Soc.* **1979**, *101*, 4374.

(57) Murray-Rust, P.; Stallings, W. C.; Monti, C. T.; Preston, R. K.; Glusker, J. P. *J. Am. Chem. Soc.* **1983**, *105*, 3206.

(58) Ramasubbu, N.; Parthasarathy, R.; Murray-Rust, P. *J. Am. Chem. Soc.* **1986**, *108*, 4308.

(59) Price, S. L.; Stone, A. J.; Lucas, J.; Rowland, R. S.; Thornley, A. E. *J. Am. Chem. Soc.* **1994**, *116*, 4910.

(60) Nyburg, S. C. *Acta Crystallogr.* **1979**, *A35*, 641.

(61) Bish, D. L., Post, J. E., Ed. *Modern Powder Diffraction*; Mineralogical Society of America: Washington, DC, 1989.

(62) Klug, H. P.; Alexander, L. E. *X-Ray Diffraction Procedures*; John Wiley & Sons: New York, 1954.

(63) The supporting information includes a figure showing the X-ray powder diffraction patterns for **1-(CH$_3$)$_2$** (||), **1-H$_2$** (×), and **1-F$_2$** (**3-D**). Each compound was crystallized under six conditions and the powder patterns were recorded and compared with the calculated pattern.

(64) Preferred orientation is well-known to cause variations in relative intensities (see refs 61 and 62).

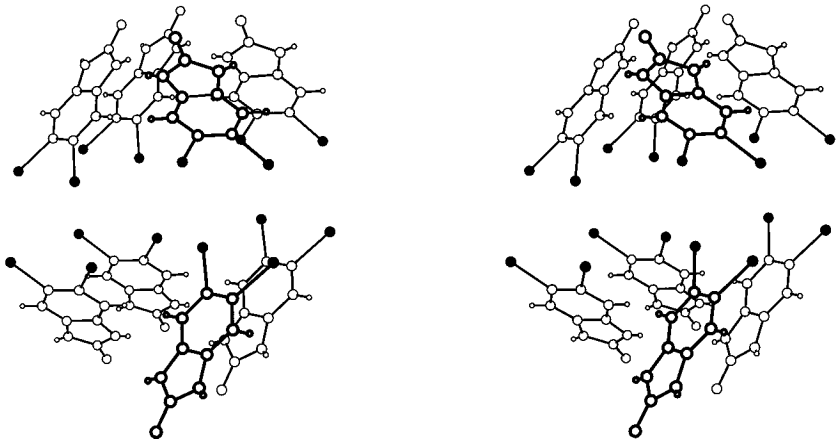

**Figure 13.** Stereoview of the asymmetric molecule of **1-I$_2$** with I···I contacts. The iodine atoms are shaded.

compounds crystallize in a well-defined minimum of free energy; we acknowledge, however, that failure to detect polymorphism does not preclude the possibility that polymorphs of these benzimidazolones exist.

## Conclusions

This work demonstrates that this series of disubstituted benzimidazolones pack in a limited set of crystalline forms (‖, ×, and **3-D**). Our results suggest that there is a propensity for the benzimidazolones to form tapes in the solid state, although the **3-D** network is preferred in some cases. In this system, the tape and the **3-D** network are competing motifs that are comparable in energy; thus, influences such as weak electrostatic interactions and interactions between halogens seem to be important in determining the motif. Although this situation complicates prediction of the motif, it has allowed us to identify some secondary intermolecular interactions (I···I and F···H contacts) that seem to influence the crystal structure. On the basis of our results, we expect that molecules with other substituents that are highly polarizable (permitting favorable VDW interactions) or polarized (permitting favorable electrostatic interactions) will crystallize in a **3-D** motif.

For the benzimidazolones that *do* form tapes, we can rationalize the packing of tapes in three dimensions only on the basis of molecular structure: the substitution at the edge of the tape determines whether the tapes crystallize in a parallel or nonparallel arrangement. Tapes of benzimidazolones without substituents at the edges tend to crystallize in the nonparallel arrangement because it fills the spaces between adjacent molecules in the tape. For the parent compound **1-H$_2$**, the nonparallel arrangement also permits a favorable electrostatic interaction between a carbon in the aromatic ring and an aromatic hydrogen from an adjacent tape. Substitution of the aromatic ring with atoms larger than hydrogen provides smooth edges that cannot intercalate in a nonparallel arrangement. This substitution also replaces aromatic hydrogens involved in the electrostatic interaction favoring the nonparallel arrangement. Thus, we have begun to define a relationship between the molecular structure and the crystal structure of benzimidazolones. Our results suggest that analysis of interactions at the edges of tapes provides the best chance for *predicting* the packing arrangement of the tapes.

Compared with the melamine/barbituric acid system, the benzimidazolone system offers several important improvements in designing the solid state. Most significantly, we believe that we can rationalize the packing of tapes of benzimidazolones on the basis of the substitution at the edge of the tapes. Whether we can *predict* the packing of new molecules still remains to be tested. Furthermore, we have successfully avoided polymorphism in the 2-benzimidazolones by eliminating the possibility for conformational isomerism. The lack of polymorphism in this system allows us to compare only structures of minimum free energy. Finally, benzimdazolones tend to crystallize as blocks or plates, rather than as the thin needles that plagued the (Bar·Mel(PhX)$_2$) system. The hydrogen bonds in the benzimidazolones are weaker and fewer in number than those in the (Bar·Mel(PhX)$_2$); thus, the rate of growth along the long axis of the tape is comparable to that in other dimensions.

One complication in this system relative to (Bar·Mel(PhX)$_2$) is that the formation of tapes is less reliable. Various interactions introduced through substituents can promote a switch from one hydrogen-bonded motif to another. In the (Bar·Mel(PhX)$_2$) system, a switch in motifs occurs to relieve steric interactions between molecules *within the tape*. In the benzimidazolones, a switch in motifs occurs to maximize electrostatic or van der Waals interactions between molecules *within the crystalline environment.* That is, there is nothing inherently unstable about the tape itself, but interactions *between* tapes are sometimes less favorable than interactions between molecules in the **3-D** motif. For the benzimidazolones, the interactions that shift the motif from tape to **3-D** can be weak and thereby complicate the prediction of the motif.

We believe that the benzimidazolones are a useful model system with which to approach structural design in the solid state. Derivatives of benzimidazolones with a wide range of substituents are relatively easy to synthesize (although the diamines from which they are derived can be synthetically challenging). Careful crystallization yields single crystals, although the low solubility of some of the compounds makes crystallization nonroutine. The simplicity (planarity, conformational rigidity, and lack of conformational polymorphism) of these molecules also makes them more amenable to computational analysis than the (Bar·Mel(PhX)$_2$) system.[65] Our results emphasize the importance of identifying the effects of secondary interaction on the structure of organic molecules in crystals.

## Experimental Section

**General Methods.** Dinitroaniline, 1,2-phenylenediamine, 4,5-dichloro-1,2-phenylenediamine, 4,5-dimethyl-1,2-phenylenediamine, 4,5-difluoro-2-nitroaniline, and 1,2-diaminonaphthalene (Aldrich), and 1,1′-carbonyldiimidazole (Sigma) were used as received without purification. Reagent-grade THF was distilled from sodium benzophenone ketyl; all other solvents were reagent grade and were used without

(65) The many torsions of the phenyl rings in the Bar·Mel(PhX)$_2$ made modelling difficult because there were multiple conformations that gave nearly isoenergetic structures. We expect computations to be most successful in systems having well-defined minima of free energy.

purification. Melting points were determined on a Mel-Temp apparatus and are uncorrected.

**Preparation of 4,5-Substituted 1,2 Phenylenediamines.** 4,5-Diiodo-1,2-phenylenediamine was prepared by nitration of dinitroaniline, followed by reduction with Sn/HCl.[66] 4,5-Difluoro-1,2-phenylenediamine was prepared by reduction of 4,5-difluoro-2-nitroaniline with $SnCl_2$/HCl.[67] 4,5-Dibromo-1,2-phenylenediamine was prepared by bromination of *N*,*N*′-bis(p-toluenesulphonyl)-*o*-phenylenediamine.[68]

**General Procedure for Carbonylation of 4,5-Substituted 1,2-Phenylenediamines.**[69] A solution of 1,1′-carbonyldiimidazole (1.2 equiv, 0.4 M in THF) was added in drops with stirring at room temperature to a solution of the appropriate diamine (1 M in THF), and the mixture was stirred for 3 days. Compounds **1-H$_2$**, **1-Cl$_2$**, **1-(CH$_3$)$_2$**, **1-Br$_2$**, **1-I$_2$**, and **2-H$_2$** precipitated from solution as they were formed and were isolated by filtration. The product was washed with THF and then dried *in vacuo*. Solutions of **1-Br$_2$**, **1-I$_2$**, and **2-H$_2$** in DMF were treated with decolorizing charcoal prior to recrystallization. Compound **1-F$_2$** was soluble in THF and did not precipitate. It was isolated by crystallization from THF/water, upon slow evaporation of THF.

**2-Benzimidazolone (1-H$_2$)**.[36] From 5.0135 g of 1,2-phenylenediamine: 2.0181 g, 47%; $^1$H NMR (400 MHz, DMSO-$d_6$) $\delta$ 10.60 (br s, 2H), 6.91 (s, 4H (two overlapping signals)); $^{13}$C NMR (100 MHz, DMSO-$d_6$) $\delta$ 160.57, 134.88, 125.70, 113.78; HRMS (M) calcd for $C_7H_6N_2O$ 134.0480, found 134.0482.

**4,5-Dimethyl-2-benzimidazolone (1-(CH$_3$)$_2$).** From 4.9924 g of 4,5-dimethyl-1,2-phenylenediamine: 1.8445 g, 44%; $^1$H NMR (400 MHz, DMSO-$d_6$) $\delta$ 10.33 (br s, 2H), 6.69 (s, 2H); $^{13}$C NMR (100 MHz, DMSO-$d_6$) $\delta$ 155.41, 127.75, 127.74, 109.54, 19.39; HRMS (M + $NH_4^+$) calcd for $C_9H_{10}N_2O$ 180.1137, found 180.1147.

**4,5-Dichloro-2-benzimidazolone (1-Cl$_2$).** From 4.5999 g of 4,5-dichloro-1,2-phenylenediamine: 2.4791 g, 52%; $^1$H NMR (400 MHz, DMSO-$d_6$) $\delta$ 10.91 (br s, 2H), 7.09 (s, 2H); $^{13}$C NMR (100 MHz, DMSO-$d_6$) $\delta$ 155.11, 129.80, 122.30, 109.70; HRMS (M) calcd for $C_7H_4Cl_2N_2O$ 201.9701, found 201.9697.

**4,5-Difluoro-2-benzimidazolone (1-F$_2$).** From 4,5-difluoro-1,2-phenylenediamine: $^1$H NMR (400 MHz, DMSO-$d_6$) $\delta$ 10.78 (br s, 2H), 6.98 (t, $J_{H-F}$ = 8.8 Hz, 2H); $^{13}$C NMR (100 MHz, DMSO-$d_6$) $\delta$ 156.05, 145.05 (d, $J_{C-F}$ = 219.9), 125.59, 98.25; HRMS ($M^+$) calcd for $C_7H_4F_2N_2O$ 170.0291, found 170.0295.

**4,5-Diiodo-2-benzimidazolone (1-I$_2$).** From 352 mg of 4,5-diiodo-1,2-phenylenediamine: 197 mg, 54%; $^1$H NMR (400 MHz, DMSO-$d_6$) $\delta$ 10.79 (br s, 2H), 7.39 (s, 2H); $^{13}$C NMR (100 MHz, DMSO-$d_6$) $\delta$ 154.59, 131.45, 118.00, 96.41; HRMS ($M^+$) calcd for $C_7H_4I_2N_2O$ 385.8413, found 385.8410.

**4,5-Dibromo-2-benzimidazolone (1-Br$_2$).** From 1.035 g of 4,5-dibromo-1,2-phenylenediamine: 0.628 g, 55%; $^1$H NMR (100 MHz, DMSO-$d_6$) $\delta$ 10.91 (br s, 2H), 7.21 (s, 2H); $^{13}$C NMR (400 MHz, DMSO-$d_6$) $\delta$ 154.99, 130.65, 113.92, 112.69; HRMS ($M^+$) calcd for $C_7H_4Br_2N_2O$ 289.8690, found 289.8701.

**2-Naphthimidazolone (2-H$_2$).** From 0.982 g of 1,2-diaminonaphthalene: 0.913 g, 80%; $^1$H NMR (100 MHz, DMSO-$d_6$) $\delta$ 10.79 (br s, 2H), 7.79 (m, 2H), 7.29 (m, 2H), 7.26 (m, 2H); $^{13}$C NMR (400 MHz, DMSO-$d_6$) $\delta$ 156.22, 131.09, 129.24, 126.85, 123.26, 103.60; HRMS ($M^+$) calcd for $C_{11}H_8N_2O$ 184.0637, found 184.0640.

**Crystallization of Single Crystals of Benzimidazolones for X-ray Crystallography. 1-H$_2$**, **1-Br$_2$**, **1-I$_2$**, and **2-H$_2$**: crystals were grown by evaporation of a solution of the compound in methanol in a beaker covered with filter paper. **1-H$_2$** gave colorless blocks (approximately 0.2 × 0.2 × 0.1 mm). **1-Br$_2$** gave colorless plates (approximately 0.02 × 0.10 . 0.02 mm). **1-I$_2$** gave colorless plates (approximately 0.35 × 0.15 × 0.03). **2-H$_2$** gave gold rods (approximately 0.15 × 0.02 × 0.02 mm). **1-(CH$_3$)$_2$** and **1-Cl$_2$**: crystals were grown by cooling warm solutions in DMF. **1-(CH$_3$)$_2$** gave gold blocks (approximately 0.25 × 0.22 × 0.10 mm). **1-Cl$_2$** gave gold blocks (approximately 0.25 × 0.07 × 0.11 mm). **1-F$_2$**: thick gold plates were grown by diffusion of diethyl ether into a solution in THF (approximately 0.35 × 0.25 × 0.08).

**Determination of Crystal Structure by X-ray Crystallography.** The details of X-ray data collection and structure solution and refinement are provided in the supporting information. Data were collected by Molecular Structure Corp., The Woodlands, TX, on a Rigaku AFC5R diffractometer equipped with a rotating anode generator. All structures were solved and refined at Harvard using the SHELXPLUS package of programs.

**X-ray Powder Diffraction.** The powder diffraction patterns were collected on a Scintag XDS 2000 diffractometer using CuK$\alpha$1 $\lambda$ 1.5405 radiation. The samples were prepared by grinding the crystals with a mortar and pestle and spreading the powder on a microscope slide.

**Computational Methods.** All energy calculations used the Drieding II parameters[50] for van der Waals interactions and electrostatic potential charges (ESP) derived from MOPAC6. Starting from the geometries of the crystal structures, MOPAC6 was used to optimize the bonds and angles. Calculations of the lattice energies were done using Cerius2. CHARMm 22[70] was used to calculate the interaction energies in these tapes using values of the VDW parameter and partial charges described above.

**Acknowledgment.** We acknowledge the support of the National Science Foundation through Grant CHE-91-22331. J.C.M. wishes to acknowledge Merck for a postdoctoral fellowship. We thank Professor Andrew Barron for helpful discussions, especially concerning X-ray powder diffraction.

**Supporting Information Available:** Crystallographic detail including tables of atomic positional parameters and bond lengths and angles (33 pages). This material is contained in many libraries on microfiche, immediately follows this article in the microfilm version of the journal, can be ordered from the ACS, and can be downloaded from the Internet; see any current masthead page for ordering information and Internet access instructions.

JA952836L

(66) Arotsky, J.; Butler, R.; Darby, A. C. *J. Chem. Soc. (C)* **1970**, 1480.
(67) Uchida, M.; Morita, S.; Chihiro, M.; Kanbe, T.; Yamasaki, K.; Yabuuchi, Y.; Nakagawa, K. *Chem. Pharm. Bull.* **1989**, *37*, 1517.
(68) Cheesman, G. W. H. *J. Chem. Soc. (C)* **1962**, 1170.
(69) Felix, A. M.; Fryer, R. I. *J. Heterocycl. Chem.* **1968**, *5*, 291.
(70) Brooks, B. R.; Bruccoleri, R. E.; Olafson, B. D.; States, D. J.; Swaminathan, S.; Karplus, M. *J. Comput. Chem.* **1983**, *4*, 187.